CHAPTER TEN

Methods to Assess Mitochondrial Morphology in Mammalian Cells Mounting Autophagic or Mitophagic Responses

S. Marchi, M. Bonora, S. Patergnani, C. Giorgi, P. Pinton[1]
Section of Pathology, Oncology and Experimental Biology, Laboratory for Technologies of Advanced Therapies (LTTA), University of Ferrara, Ferrara, Italy
[1]Corresponding author: e-mail address: paolo.pinton@unife.it

Contents

Abstract

It is widely acknowledged that mitochondria are highly active structures that rapidly respond to cellular and environmental perturbations by changing their shape, number, and distribution. Mitochondrial remodeling is a key component of diverse biological

processes, ranging from cell cycle progression to autophagy. In this chapter, we describe different methodologies for the morphological study of the mitochondrial network. Instructions are given for the preparation of samples for fluorescent microscopy, based on genetically encoded strategies or the employment of synthetic fluorescent dyes. We also propose detailed protocols to analyze mitochondrial morphometric parameters from both three-dimensional and bidimensional datasets. Finally, we describe a protocol for the visualization and quantification of mitochondrial structures through electron microscopy.

1. INTRODUCTION

Mitochondria are highly dynamic organelles that often change shape and intracellular distribution during their life course. Both number and morphology of mitochondria are regulated by specifically controlled rates of organelle fusion and fission (Chan, 2012; Youle & van der Bliek, 2012). Therefore, the molecular machinery involved in the control of mitochondrial dynamics include both proteins responsible of mitochondrial fusion, such as the outer mitochondrial membrane proteins mitofusin 1 (Mfn1) and mitofusin 2 (Mfn2) (Santel & Fuller, 2001) and the inner membrane protein optic atrophy 1 (Opa1) (Meeusen et al., 2006), and pro-fission factors, such as dynamin-related protein 1 (Drp1) (Bleazard et al., 1999), Fis1 (Yoon, Krueger, Oswald, & McNiven, 2003), and the mitochondrial fission factor (Mff) (Otera et al., 2010). A high number of papers have described dramatic remodeling of the mitochondrial network during a wide range of pathophysiological conditions, which include differentiation (Kasahara & Scorrano, 2014), cell cycle progression (Mitra, Wunder, Roysam, Lin, & Lippincott-Schwartz, 2009), mitochondrial respiratory chain function (Benard & Rossignol, 2008), Ca^{2+} transfer (Szabadkai et al., 2004), apoptosis (Karbowski & Youle, 2003; Morciano, Pedriali, et al., 2016), and autophagy (Galluzzi et al., 2015; Okamoto & Kondo-Okamoto, 2012). Upon autophagy induction by nutrient depletion, mitochondria seem to elongate in order to supply ATP in times of starvation, especially at early phases of the autophagic process (Gomes, Di Benedetto, & Scorrano, 2011; Rambold, Kostelecky, Elia, & Lippincott-Schwartz, 2011). Conversely, it is widely accepted as mitochondrial fragmentation events occurred before selective clearance of mitochondria by mitophagy, which allowed the engulfment of damaged and potentially harmful mitochondria into autophagosomes (Rimessi et al., 2013). Thus, changes in mitochondrial

morphology represented a key aspect in the regulation of both autophagy and mitophagy. Here, we describe different assays for monitoring and quantifying the state of the mitochondrial network before and after autophagy/mitophagy induction. Importantly, most of these methods can be exploited for morphometric analyses of the mitochondrial compartment that might occur upon stimuli of various nature or different pathological contexts.
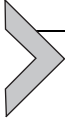
2. HIGH-RESOLUTION IMAGING OF MITOCHONDRIA IN LIVE CELLS BASED ON FLUORESCENT PROTEIN VARIANTS

The proposed protocol allows the measurement of mitochondrial morphology and dynamics with recombinant variants of the green fluorescent protein (GFP), obtained from jellyfish *Aequorea victoria* in the early 1990s (Heim & Tsien, 1996). Optimal analysis of mitochondrial network is primary obtained by using a mitochondrially targeted GFP (mtGFP) (Rizzuto et al., 1998) or a monomeric red fluorescent protein mCherry fused with the mitochondrial target sequence from subunit VIII of human cytochrome *c* oxidase (mCherry-Mito-7; Addgene plasmid #55102) (Olenych, Claxton, Ottenberg, & Davidson, 2007).

2.1 Equipment Setup

Mitochondrial structures could be imaged and recorded by using a spinning disk confocal microscope (or equivalent competitors) equipped with the appropriate filter set. The system should be set in order to reach a configuration as close as possible to the Nyquist rate (https://svi.nl/Nyquistcalculator). Typically, correct sampling can be achieved by using $60 \times$ lens or higher with numerical aperture (N.A.) > 1.3, and high-resolution CCD or CMOS cameras (with pixel size $< 8\ \mu m$). In this protocol, we will illustrate experiments performed on a Nikon LiveScan Swept Field Confocal Microscope (SFC) Eclipse Ti with a $60 \times$ magnification and equipped with NIS-Elements microscope imaging software (Nikon Instruments, Melville, NY, USA) and Andor iXon EM-CCD camera (Belfast, Northern Ireland) (Marchi et al., 2015; Patergnani et al., 2013).

2.2 Reagents Setup

- Transfection reagents.
- Dulbecco's Modified Eagle Medium (DMEM) supplemented of FBS 10% or Modified Krebs–ringer solution (KRB): 125 m*M* NaCl,

5 mM KCl, 1 mM KH$_2$PO$_4$, 1 mM MgSO$_4$, 1 mM CaCl$_2$, 5.5 mM glucose, and 20 mM HEPES, pH 7.4.

- Glass coverslips 24 mm in diameter.
- Attofluor chamber for microscopy with stage holder for mounting.

2.3 Sample Preparation and Transfection

The cells are seeded on glass coverslips (24 mm in diameter) and allowed to grow until 50% confluence. After seeding the cells, wait at least 24 h. The cells are then transfected using appropriate transfection methods with mitochondrially targeting fluorescent proteins.

Conventionally cancerous and immortalized cell lines may be easily transfect with Ca^{2+}-phosphate or lipoamines transfection methods. Primary cultures, which are notably "hard-to-transfect cells," request electroporation or adenoviral vectors. Cultures obtained from human beings may be reluctant to the transfection. In order to perform mitochondrial network analysis in these cell samples, please refer to Section 4.

2.4 Measurements

- Mount the glass coverslips into the Attofluor chamber and add 500–1000 μL of DMEM or KRB.
- Place the chamber on the 37°C thermo-controlled stage of the microscope.
- Prepare the appropriate camera setting. For high–resolution imaging, we recommend to use the standard binning mode 1×1 (meaning that each logical pixel is equal to one physical pixel) and to collect a z-stack of images (commonly 51) at 0.2 μm each, in order to capture the whole mitochondrial network of the cell. *Important note:* in case of low speed microscope system or highly flat cells, the operator might avoid capturing z-stacks of the images, thereby limiting the acquisitions to a single plan. In such case, see Section 4.2 for quantification of the results.
- Acquire images in multiple points mode by using motorized stage. If microscope is not equipped, record single–point pictures. We recommend to store all acquisitions with the same settings, for both camera and microscope. In order to obtain statistical significance, a number of at least 40–50 images per condition should be collected.
- Stop the analysis system, remove the chamber from the microscope stage, and clean well the objective from the immersion medium.

- Clean well the Attofluor chamber with 70% ethanol and then with Milli–Q water, before perform a new experiment.
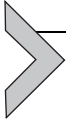
3. HIGH-RESOLUTION IMAGING OF MITOCHONDRIAIN LIVE CELLS WITH MITOCHONDRIAL-SPECIFIC FLUORESCENT DYES

The very limited photobleaching of GFP provides the primary advantage of the fluorescent protein over the dyes. Nevertheless, the employment of such plasmids is not always possible. Several primary cultures are reluctant to the transfection with the conventional methods (including electroporation and viral vectors). The main cell populations "hard–to–transfect cells" are those obtained from human beings, such as fibroblasts. Considering this aspect, alternative approaches to stain the mitochondrial network of these cells are needed. We propose a detailed protocol aimed to describe the use of the most common mitochondrial fluorescent chemical probes to analyze mitochondrial dynamics and network.

3.1 Equipment and Reagents Setup

- Confocal microscope (please refer to Section 2.1).
- Mitochondrial fluorescent dyes: MitoTracker Green, MitoTracker Orange, MitoTracker Red, and MitoTracker Deep Red versions.

3.2 Reagents Setup

- DMEM supplemented of FBS 10% (DMEM) or Modified KRB: 125 mM NaCl, 5 mM KCl, 1 mM KH$_2$PO$_4$, 1 mM MgSO$_4$, 1 mM CaCl$_2$, 5.5 mM glucose, and 20 mM HEPES, pH 7.4.
- Glass coverslips 24 mm in diameter.
- Attofluor chamber for microscopy with standard 35–mm diameter stage holder for mounting.
- MitoTracker dyes. We recommend preparing a stock solution in a range of 100–500 μM. Working solution may be utilized up to 1–2 months and conserved at −20°C.

3.3 Sample Preparation and Measurements

- Seed the cells on glass coverslips (24 mm in diameter) and allow them to reach 50–70% confluence. After seeding cells, wait at least 24 h.
- Load the cells with an appropriate MitoTracker dye in agreement with the microscope filter setting available. We recommend using the probes

at final concentration in a range of 1–100 nM. The appropriate final concentration depends on cell type and should be achieved by the operator. To obtain an optimal dye loading, we suggest to incubate cells for 30–60 min at 37°C, 5% CO_2.

- Wash cells with KRB or DMEM for at least three times.
- Mount the glass coverslips into the Attofluor chamber and add 500–1000 μL of DMEM or KRB.
- Place the chamber on the 37°C thermo-controlled stage of the microscope.
- Prepare the appropriate camera setting. For high-resolution imaging, we recommend to use the standard binning mode 1×1 (meaning that each logical pixel is equal to one physical pixel) and collect a z-stack of images (commonly 51) at 0.2 μm each, in order to capture the whole mitochondrial network of the cell. *Important note:* in case of low speed microscope system or highly flat cells, the operator might avoid capturing z-stacks of the images, thereby limiting the acquisitions to a single plan. In such case, see Section 4.2 for quantification of the results.
- Acquire images in multiple points mode by using motorized stage. If microscope is not equipped, record single-point pictures. We recommend storing all acquisitions with the same settings, for both camera and microscope. In order to obtain statistical significance, a number of at least 40–50 images per condition should be collected.
- Stop the analysis system, remove the chamber from the microscope stage, and clean well the objective from the immersion medium.
- Clean well the Attofluor chamber with 70% ethanol and then with Milli-Q water, before starting a new experiment.

Notes:
- Mitochondrial structures may be also imaged and recorded after fixation procedures. Several fixatives are available. The most common are aldehydes (such as formaldehyde or glutaraldehyde) and organic solvents, such as methanol, ethanol, and acetone. Among them, we recommended to fix cells with paraformaldehyde (PFA). The optimal PFA concentration depends from the cellular type. We suggest to use 4% PFA for immortalized cells and 2% for primary cells.
- It is very important to consider that not all chemical probes staining the mitochondrial population are retained after fixation procedures. For fixed cells, we recommend using MitoTracker Orange or MitoTracker Deep Red versions. Such fluorescent dyes are well retained after aldehyde fixation.

- All the mitochondrial fluorescent dyes reported here are very sensitive to variations in mitochondrial membrane potential (MMP). Thus, when using compounds that could induce autophagy/mitophagy through perturbation of the MMP, such as Antimycin A or FCCP (carbonyl cyanide-4-(trifluoromethoxy)phenylhydrazone), we suggest to mark the mitochondrial compartment through antibodies raised against highly expressed mitochondrial proteins, rather than using fluorescent chemical compounds. We propose four antibodies that work very well in immunofluorescence technique and could allow a reliable quantification of the mitochondrial morphology:

    1. Anti–TOM20 [outer mitochondrial membrane protein; Santa Cruz Biotechnology (Santa Cruz, CA, USA) (sc-11415); dilution: 1:100–1:1000].
    2. Anti–HSP60 [matrix protein; Santa Cruz Biotechnology (sc–13115); dilution: 1:100–1:1000].
    3. Anti–TIM23 [mitochondrial inner membrane protein; BD Transduction Laboratories (Franklin Lakes, NJ, USA) (code: 611222); dilution: 1:100].
    4. Anti–ATP5B [matrix protein; Millipore (Darmstadt, Germany) (MAB3494); dilution: 1:100–1:1000].
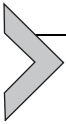
4. ANALYSIS OF THE RESULTS

4.1 Analysis of Mitochondrial Morphology on a Three-Dimensional Dataset (Fig. 1)

- Open Fiji software (Schindelin et al., 2012) and load the files output from microscope software.
- Denoise images by applying a Gaussian filter with dimension size of 1 pixel (Menu Process → Filters → Gaussian…).
- Remove background setting the rolling ball to a size of approximately 1 μm (Menu Process → Subtract Background…).
- Generate segmented image (Menu Analyze → 3D Objects Counter). An automated threshold algorithm will find the best threshold value, nonetheless this could require minor adjustment to include all the mitochondria. Set the filters to a minimum of 8 pixels to a maximum of 1,000,000 pixels. Check the option "Statistics." A result table will appear.
- Collect the volume measurement column in a spreadsheet file and calculate average volume (average mitochondrial size), the sum of all the volume (mitochondrial content), and number of objects (mitochondrial counts).
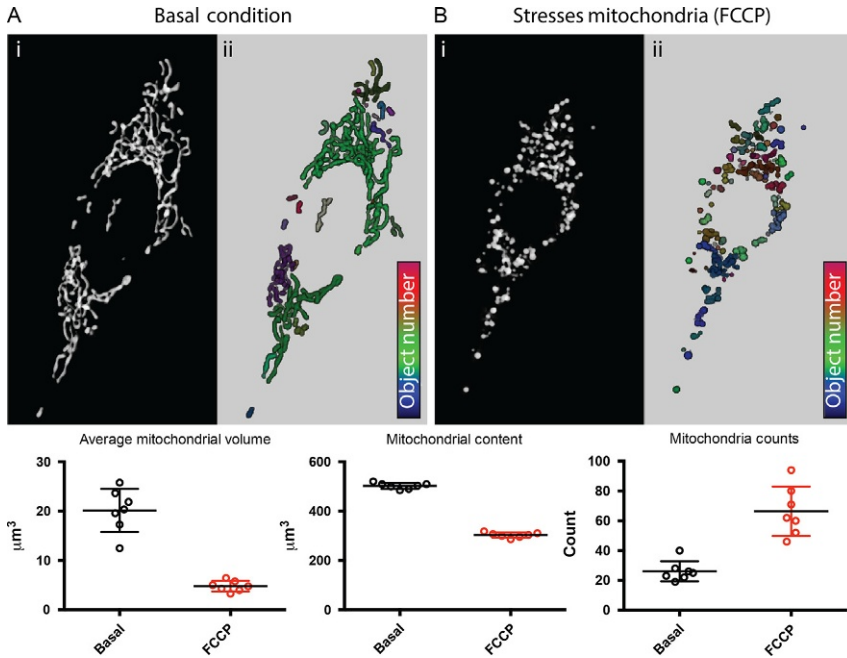
Fig. 1 Representative volume render (Ai and Bi) and segmented image (Aii and Bii) of mitochondrial network derived from mtGFP expressing CHO cells during basal conditions (A) or after FCCP exposure (B).

- Repeat the procedure for all the collected samples.
- Generate three data table, for independent collection of the three measurements.
- Choose the appropriate statistical method to compare volume measurement and object number within groups. A list of the different outputs that could arise from the analysis and of the mitochondrial processes that are associated to the morphological rearrangements are showed in Table 1.

Notes: The present procedure refers to the open source software for image analysis Fiji. Comparable results could be obtained with other open source (e.g., Icy) or commercial available software (e.g., Bitplane Imaris, Perkin Elmer Volocity).

4.2 Analysis of Mitochondrial Morphology on a Bidimensional Dataset (Fig. 2)

- Open Fiji software (Schindelin et al., 2012) and load the files output from microscope software.

Table 1 Representative Interpretation of Most Common Phenotypes That Could Be Associated to Different Processes That Regulate Mitochondrial Morphology

Process	Observed Phenotype	Refs.
Mitochondrial fission	Increase in mitochondrial counts and reduction in average mitochondrial size	Bonora et al. (2013)
Mitochondrial fusion	Reduction in mitochondrial counts and increase in average mitochondrial size	Morciano, Giorgi, et al. (2016)
Mitophagy	Reduction in mitochondrial content and reduction in average mitochondrial size	Sumpter et al. (2016)
Mitochondrial biogenesis	Increase in mitochondrial content and increase in average mitochondrial size (not always)	Bianchi et al. (2006)

- Denoise images by applying a Gaussian filter with dimension size of 1 pixel (Menu Process → Filters → Gaussian…).
- Remove Background setting the rolling ball to a size of approximately 1 µm (Menu Process → Subtract Background…).
- Threshold image to isolate mitochondria from background (Menu Image → Adjust → Threshold…). Choose the most appropriate thresholding algorithms (usually "Otsu" or "Triangle" are the most performing).
- Set measurement type (Menu Analyze → Set measurements…). Check the options "Area," "Perimeter," "Feret's diameter," "Limit to threshold").
- Measure mitochondria (Menu Analyze → Analyze particles). Set a minimum filter size to 2, check the "Pixel units," and "Display results" options.
- Collect the measurement columns in a spreadsheet file and calculate the aspect ratio and form factor according to equations displayed in Fig. 2Bi
- Repeat the procedure for all the collected samples.
- Generated three data table, for independent collection of the three measurements.
- Choose the appropriate statistical method to compare form indexes.

Notes:

The thresholding method should not be modified between samples.

The present procedure refers to the open source software for image analysis Fiji. Comparable results could be obtained with other open source (e.g., Icy) or commercial available software (e.g., Molecular Devices Metamorph, Perkin Elmer Volocity, Nikon NIS-Elements, Zeiss Zen, Leica LAS X).
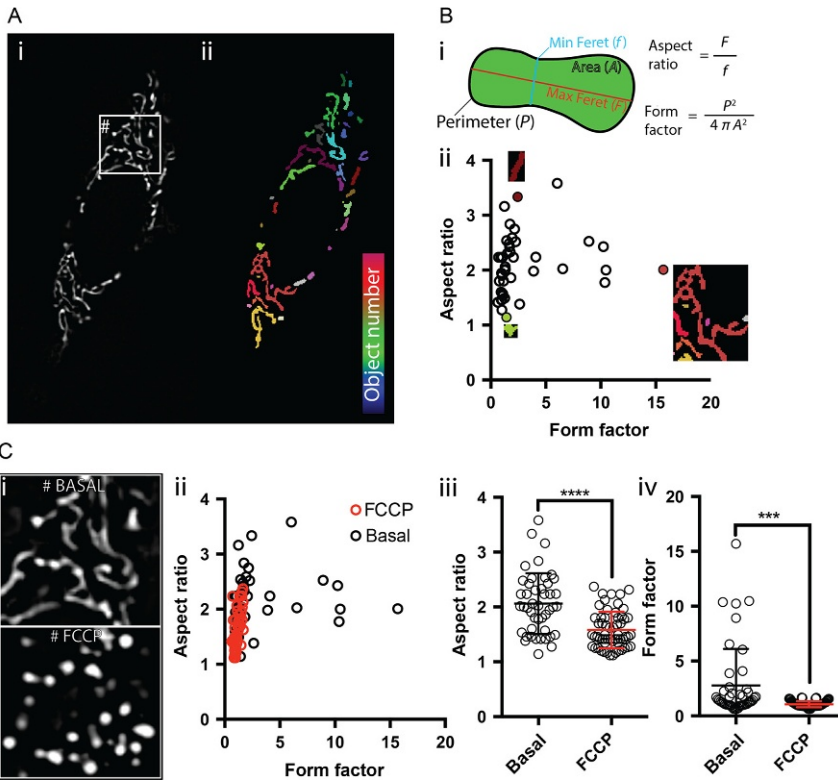
Fig. 2 Representative confocal section (Ai) and segmented image (Aii) of mitochondrial network in mtGFP expressing CHO cells during basal conditions. Diagrammatic representation of morphological meaning of aspect ratio and form factor indexes (Bi) and relative distribution in scatter plot (Bii). Zoom image of inset from image (Ai) before and after administration of FCCP (Ci). Representative scatter plot of form indexes distribution before and after FCCP administration (Cii) also statistical analysis of both indexes are displayed in (Ciii) and (Civ) (***$p < 0.005$ and ****$p < 0.001$ for Student's T-test).
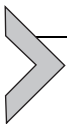
5. ASSESSMENT OF MITOCHONDRIAL MORPHOLOGY USING ELECTRON MICROSCOPY

The proposed protocol is referred to cells grown in culture dishes. The same protocol could be exploited also to cells in suspension or tissue sections. Notably, a detailed protocol for determination of mitochondrial ultrastructures in tissue samples by electron microscopy (EM) has been described by Sasaki (2010).

For the visualization of mitochondrial structure, we suggest the employment of a transmission electron microscope (TEM), with a magnification of at least $20,000 \times$.

5.1 Reagents Setup

- Fixative: 2% glutaraldehyde and 0.1 M sodium cacodylate, pH 7.4.
- 1% Osmium tetroxide (OsO_4), freshly prepared.
- 0.1 M Sodium cacodylate, pH 7.4, kept at room temperature (RT) for up to 6 months.
- Ethanol at different percentages, all stored at 4°C.

5.2 Sample Preparation

- Seed cells on 3- or 6-cm culture dishes and allow cells to grow until reach approximately 70% confluence. You should obtain a visible pellet, reaching an approximate volume of 10–30 μL.
- Fix cells with 2% (w/v) glutaraldehyde buffered with 0.1 M sodium cacodylate, pH 7.4, for 2 h at RT.
- Carefully detach the fixed cells using a plastic cell scraper.
- Collect the cells into Eppendorf tubes, and centrifuge (5 min at $500 \times g$) to obtain the pellet.
- Wash three times with 0.1 M sodium cacodylate, pH 7.4.
- Postfix the pellets in 1% osmium tetroxide at RT for 1 h.
- Wash three times in distilled water.
- Stain with 0.5% uranyl acetate overnight at 4°C.
- Dehydrate the pellets in graded steps of ethanol (50%, 70%, 90%, and 100%) two times with 100% acetone (each of 15–30 min at 4°C).
- Embed the pellets into Epon™ (Sigma–Aldrich).
- Cut sections (60 nm thick) using an ultramicrotome.
- Electron microscopy examination.

5.3 Analysis of EM Images

The first critical step in quantitative microscopy is sampling, which must absolutely be unbiased. Moreover, every region of the sample should have an equal chance to be included in the counting, based on the principle of uniform random sampling (Yla-Anttila, Vihinen, Jokitalo, & Eskelinen, 2009). Due to the peculiar architecture of mitochondria, a double-membrane system with a wide cristae compartment, is quite easy to manually annotate mitochondrial regions on EM images. However, auto-mated or semiautomatic methods that allow both shape information and regional statistics to segment mitochondria in EM images have been recently described (Higaki et al., 2015; Seyedhosseini, Ellisman, & Tasdizen, 2013).

The analysis of mitochondrial compartments on EM samples could be carried out manually or through the support of ImageJ (or Fiji) software.

A manual quantification of mitochondrial morphology is based on their appearance, especially referring to the shape of mitochondrial cristae. Four degrees of mitochondrial conformations have been proposed to classify the state and healthy of the organelles (Cogliati, Enriquez, & Scorrano, 2016; Rimessi et al., 2015; Scorrano et al., 2002). This classification includes

- Class I mitochondria: normal mitochondria with a well-defined outer membrane and a numerous narrow pleomorphic cristae (appearing in TEM as small electron-transparent areas) in a contiguous electron-dense matrix space.
- Class II mitochondria: remodeled mitochondria with widen cristae junctions with a serpentine electron-transparent intracristal compartment interrupted by electron-dense matrix spaces.
- Class III mitochondria: evident morphological defects, with partial rupture of the outer membrane.
- Class IV mitochondria: High morphological derangements, consisting in definitively swollen and ruptured mitochondria with undistinguishable cristae structure.

Morphological parameters of mitochondria in EM images could be also analyzed using the ImageJ software, as described by Picard et al. to characterize and quantify the differences in morphological descriptors of subsarcolemmal and intermyofibrillar mitochondria (Picard, White, & Turnbull, 2013). This analysis includes the assessment of the major mitochondrial shape factors (please refer to Section 4.2 and Fig. 2), such as Feret's diameter (representing the longest distance, expressed in μm, between any two points within a given mitochondrion), aspect ratio (measure of length), form factor (reflecting the complexity and branching aspect of mitochondria), and perimeter.
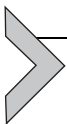
6. SUMMARY

In the last years, numerous findings sustained the close relationship existing between mitochondria and autophagy (Okamoto & Kondo-Okamoto, 2012; Sica et al., 2015). Alterations in the molecular mechanisms that regulate autophagy could result in mitochondrial remodeling and, at the same time, disturbance in mitochondrial homeostasis could contribute to malfunction of autophagy. The mutual regulation between the two processes finds its higher expression when we focus on the morphological changes that occur at mitochondrial level. Indeed, MEFs depleted for Drp1, which displayed a mitochondrial hyperfused state, strongly suppressed Parkin-mediated degradation of depolarized mitochondria (Tanaka et al.,

2010). Accordingly, liver-specific *Atg7*-knockout and systematically mosaic *Atg5*-deficient mice showed mitochondrial swelling and decreased respiration (Inami et al., 2011; Takamura et al., 2011). Again, loss of AMPK or ULK1 in liver cells resulted in accumulation of aberrant mitochondria (Egan et al., 2011). Therefore, a meticulous analysis of the mitochondrial network is required to understand the pivotal role of mitochondria in the regulation of the autophagic process or if pathological conditions that are characterized by altered autophagy could be worsened by deregulation of the mitochondrial compartment.

ACKNOWLEDGMENTS

REFERENCES

Benard, G., & Rossignol, R. (2008). Ultrastructure of the mitochondrion and its bearing on function and bioenergetics. *Antioxidants & Redox Signaling*, *10*(8), 1313–1342. http://dx.doi.org/10.1089/ars.2007.2000.

Bianchi, K., Vandecasteele, G., Carli, C., Romagnoli, A., Szabadkai, G., & Rizzuto, R. (2006). Regulation of Ca^{2+} signalling and Ca^{2+}-mediated cell death by the transcriptional coactivator PGC-1alpha. *Cell Death and Differentiation*, *13*(4), 586–596. http://dx.doi.org/10.1038/sj.cdd.4401784.

Bleazard, W., McCaffery, J. M., King, E. J., Bale, S., Mozdy, A., Tieu, Q., … Shaw, J. M. (1999). The dynamin-related GTPase Dnm1 regulates mitochondrial fission in yeast. *Nature Cell Biology*, *1*(5), 298–304. http://dx.doi.org/10.1038/13014.

Bonora, M., Bononi, A., De Marchi, E., Giorgi, C., Lebiedzinska, M., Marchi, S., … Pinton, P. (2013). Role of the c subunit of the FO ATP synthase in mitochondrial permeability transition. *Cell Cycle*, *12*(4), 674–683. http://dx.doi.org/10.4161/cc.23599.

Chan, D. C. (2012). Fusion and fission: Interlinked processes critical for mitochondrial health. *Annual Review of Genetics*, *46*, 265–287. http://dx.doi.org/10.1146/annurev-genet-110410-132529.

Cogliati, S., Enriquez, J. A., & Scorrano, L. (2016). Mitochondrial cristae: Where beauty meets functionality. *Trends in Biochemical Sciences*, *41*(3), 261–273. http://dx.doi.org/10.1016/j.tibs.2016.01.001.

Egan, D. F., Shackelford, D. B., Mihaylova, M. M., Gelino, S., Kohnz, R. A., Mair, W., … Shaw, R. J. (2011). Phosphorylation of ULK1 (hATG1) by AMP-activated protein kinase connects energy sensing to mitophagy. *Science*, *331*(6016), 456–461. http://dx.doi.org/10.1126/science.1196371.

Galluzzi, L., Pietrocola, F., Bravo-San Pedro, J. M., Amaravadi, R. K., Baehrecke, E. H., Cecconi, F., … Kroemer, G. (2015). Autophagy in malignant transformation and cancer

progression. *The EMBO Journal*, *34*(7), 856–880. http://dx.doi.org/10.15252/embj.201490784.

Gomes, L. C., Di Benedetto, G., & Scorrano, L. (2011). During autophagy mitochondria elongate, are spared from degradation and sustain cell viability. *Nature Cell Biology*, *13*(5), 589–598. http://dx.doi.org/10.1038/ncb2220.

Heim, R., & Tsien, R. Y. (1996). Engineering green fluorescent protein for improved brightness, longer wavelengths and fluorescence resonance energy transfer. *Current Biology*, *6*(2), 178–182.

Higaki, T., Kutsuna, N., Akita, K., Sato, M., Sawaki, F., Kobayashi, M., … Hasezawa, S. (2015). Semi-automatic organelle detection on transmission electron microscopic images. *Scientific Reports*, *5*, 7794. http://dx.doi.org/10.1038/srep07794.

Inami, Y., Waguri, S., Sakamoto, A., Kouno, T., Nakada, K., Hino, O., … Komatsu, M. (2011). Persistent activation of Nrf2 through p62 in hepatocellular carcinoma cells. *The Journal of Cell Biology*, *193*(2), 275–284. http://dx.doi.org/10.1083/jcb.201102031.

Karbowski, M., & Youle, R. J. (2003). Dynamics of mitochondrial morphology in healthy cells and during apoptosis. *Cell Death and Differentiation*, *10*(8), 870–880. http://dx.doi.org/10.1038/sj.cdd.4401260.

Kasahara, A., & Scorrano, L. (2014). Mitochondria: From cell death executioners to regulators of cell differentiation. *Trends in Cell Biology*, *24*(12), 761–770. http://dx.doi.org/10.1016/j.tcb.2014.08.005.

Marchi, S., Corricelli, M., Trapani, E., Bravi, L., Pittaro, A., Delle Monache, S., … Pinton, P. (2015). Defective autophagy is a key feature of cerebral cavernous malformations. *EMBO Molecular Medicine*, *7*(11), 1403–1417. http://dx.doi.org/10.15252/emmm.201505316.

Meeusen, S., DeVay, R., Block, J., Cassidy-Stone, A., Wayson, S., McCaffery, J. M., & Nunnari, J. (2006). Mitochondrial inner-membrane fusion and crista maintenance requires the dynamin-related GTPase Mgm1. *Cell*, *127*(2), 383–395. http://dx.doi.org/10.1016/j.cell.2006.09.021.

Mitra, K., Wunder, C., Roysam, B., Lin, G., & Lippincott-Schwartz, J. (2009). A hyperfused mitochondrial state achieved at G1-S regulates cyclin E buildup and entry into S phase. *Proceedings of the National Academy of Sciences of the United States of America*, *106*(29), 11960–11965. http://dx.doi.org/10.1073/pnas.0904875106.

Morciano, G., Giorgi, C., Balestra, D., Marchi, S., Perrone, D., Pinotti, M., & Pinton, P. (2016). Mcl-1 involvement in mitochondrial dynamics is associated with apoptotic cell death. *Molecular Biology of the Cell*, *27*(1), 20–34. http://dx.doi.org/10.1091/mbc.E15-01-0028.

Morciano, G., Pedriali, G., Sbano, L., Iannitti, T., Giorgi, C., & Pinton, P. (2016). Intersection of mitochondrial fission and fusion machinery with apoptotic pathways: Role of Mcl-1. *Biology of the Cell*, *108*, 279–293. http://dx.doi.org/10.1111/boc.201600019.

Okamoto, K., & Kondo-Okamoto, N. (2012). Mitochondria and autophagy: Critical interplay between the two homeostats. *Biochimica et Biophysica Acta*, *1820*(5), 595–600. http://dx.doi.org/10.1016/j.bbagen.2011.08.001.

Olenych, S. G., Claxton, N. S., Ottenberg, G. K., & Davidson, M. W. (2007). The fluorescent protein color palette. *Current Protocols in Cell Biology*, *5*, 1–34. http://dx.doi.org/10.1002/0471143030.cb2105s36. Chapter 21, Unit 21.

Otera, H., Wang, C., Cleland, M. M., Setoguchi, K., Yokota, S., Youle, R. J., & Mihara, K. (2010). Mff is an essential factor for mitochondrial recruitment of Drp1 during mitochondrial fission in mammalian cells. *The Journal of Cell Biology*, *191*(6), 1141–1158. http://dx.doi.org/10.1083/jcb.201007152.

Patergnani, S., Marchi, S., Rimessi, A., Bonora, M., Giorgi, C., Mehta, K. D., & Pinton, P. (2013). PRKCB/protein kinase C, beta and the mitochondrial axis as

key regulators of autophagy. *Autophagy*, *9*(9), 1367–1385. http://dx.doi.org/10.4161/auto.25239.

Picard, M., White, K., & Turnbull, D. M. (2013). Mitochondrial morphology, topology, and membrane interactions in skeletal muscle: A quantitative three-dimensional electron microscopy study. *Journal of Applied Physiology (Bethesda, Md.: 1985)*, *114*(2), 161–171. http://dx.doi.org/10.1152/japplphysiol.01096.2012.

Rambold, A. S., Kostelecky, B., Elia, N., & Lippincott-Schwartz, J. (2011). Tubular network formation protects mitochondria from autophagosomal degradation during nutrient starvation. *Proceedings of the National Academy of Sciences of the United States of America*, *108*(25), 10190–10195. http://dx.doi.org/10.1073/pnas.1107402108.

Rimessi, A., Bezzerri, V., Patergnani, S., Marchi, S., Cabrini, G., & Pinton, P. (2015). Mitochondrial Ca^{2+}-dependent NLRP3 activation exacerbates the *Pseudomonas aeruginosa*-driven inflammatory response in cystic fibrosis. *Nature Communications*, *6*, 6201. http://dx.doi.org/10.1038/ncomms7201.

Rimessi, A., Bonora, M., Marchi, S., Patergnani, S., Marobbio, C. M., Lasorsa, F. M., & Pinton, P. (2013). Perturbed mitochondrial Ca^{2+} signals as causes or consequences of mitophagy induction. *Autophagy*, *9*(11), 1677–1686. http://dx.doi.org/10.4161/auto.24795.

Rizzuto, R., Pinton, P., Carrington, W., Fay, F. S., Fogarty, K. E., Lifshitz, L. M., … Pozzan, T. (1998). Close contacts with the endoplasmic reticulum as determinants of mitochondrial Ca^{2+} responses. *Science*, *280*(5370), 1763–1766.

Santel, A., & Fuller, M. T. (2001). Control of mitochondrial morphology by a human mitofusin. *Journal of Cell Science*, *114*(Pt. 5), 867–874.

Sasaki, S. (2010). Determination of altered mitochondria ultrastructure by electron microscopy. *Methods in Molecular Biology*, *648*, 279–290. http://dx.doi.org/10.1007/978-1-60761-756-3_19.

Schindelin, J., Arganda-Carreras, I., Frise, E., Kaynig, V., Longair, M., Pietzsch, T., … Cardona, A. (2012). Fiji: An open-source platform for biological-image analysis. *Nature Methods*, *9*(7), 676–682. http://dx.doi.org/10.1038/nmeth.2019.

Scorrano, L., Ashiya, M., Buttle, K., Weiler, S., Oakes, S. A., Mannella, C. A., & Korsmeyer, S. J. (2002). A distinct pathway remodels mitochondrial cristae and mobilizes cytochrome c during apoptosis. *Developmental Cell*, *2*(1), 55–67.

Seyedhosseini, M., Ellisman, M. H., & Tasdizen, T. (2013). Segmentation of mitochondria in electron microscopy images using algebraic curves. *Proceedings/IEEE International Symposium on Biomedical Imaging: From Nano to Macro*, *2013*, 860–863. http://dx.doi.org/10.1109/ISBI.2013.6556611.

Sica, V., Galluzzi, L., Bravo-San Pedro, J. M., Izzo, V., Maiuri, M. C., & Kroemer, G. (2015). Organelle-specific initiation of autophagy. *Molecular Cell*, *59*(4), 522–539. http://dx.doi.org/10.1016/j.molcel.2015.07.021.

Sumpter, R., Jr., Sirasanagandla, S., Fernandez, A. F., Wei, Y., Dong, X., Franco, L., … Levine, B. (2016). Fanconi anemia proteins function in mitophagy and immunity. *Cell*, *165*(4), 867–881. http://dx.doi.org/10.1016/j.cell.2016.04.006.

Szabadkai, G., Simoni, A. M., Chami, M., Wieckowski, M. R., Youle, R. J., & Rizzuto, R. (2004). Drp-1-dependent division of the mitochondrial network blocks intraorganellar Ca^{2+} waves and protects against Ca^{2+}-mediated apoptosis. *Molecular Cell*, *16*(1), 59–68. http://dx.doi.org/10.1016/j.molcel.2004.09.026.

Takamura, A., Komatsu, M., Hara, T., Sakamoto, A., Kishi, C., Waguri, S., … Mizushima, N. (2011). Autophagy-deficient mice develop multiple liver tumors. *Genes & Development*, *25*(8), 795–800. http://dx.doi.org/10.1101/gad.2016211.

Tanaka, A., Cleland, M. M., Xu, S., Narendra, D. P., Suen, D. F., Karbowski, M., & Youle, R. J. (2010). Proteasome and p97 mediate mitophagy and degradation of

mitofusins induced by Parkin. *The Journal of Cell Biology*, *191*(7), 1367–1380. http://dx. doi.org/10.1083/jcb.201007013.

Yla-Anttila, P., Vihinen, H., Jokitalo, E., & Eskelinen, E. L. (2009). Monitoring autophagy by electron microscopy in Mammalian cells. *Methods in Enzymology*, *452*, 143–164. http://dx.doi.org/10.1016/S0076-6879(08)03610-0.

Yoon, Y., Krueger, E. W., Oswald, B. J., & McNiven, M. A. (2003). The mitochondrial protein hFis1 regulates mitochondrial fission in mammalian cells through an interaction with the dynamin-like protein DLP1. *Molecular and Cellular Biology*, *23*(15), 5409–5420.

Youle, R. J., & van der Bliek, A. M. (2012). Mitochondrial fission, fusion, and stress. *Science*, *337*(6098), 1062–1065. http://dx.doi.org/10.1126/science.1219855.